

Optical Properties of Monolayer Bismuthene in Electric Fields

Rong-Bin Chen^{1,*}, Der-Jun Jang², Ming-Chieh Lin^{3,*}, and Ming-Fa Lin^{4,*}

¹Center of General Studies, National Kaohsiung Marine University, Kaohsiung 811, Taiwan

²Department of Physics, National Sun Yat-Sen University, Kaohsiung 804, Taiwan

³Department of Electrical and Biomedical Engineering, Hanyang University, Seoul 04763, Korea

⁴Department of Physics, National Cheng Kung University, Tainan 701, Taiwan

Abstract

Optical excitations of monolayer bismuthene present the rich and unique absorption spectra. The threshold frequency is not equal to an indirect energy gap, and it becomes zero under the critical electric field. The frequency, number, intensity and form of the absorption structures are dramatically changed by the external field. The prominent peaks and the observable shoulders, respectively, arise from the constant-energy loop and the band-edge states of parabolic dispersions. These directly reflect the unusual electronic properties, being very different from those in monolayer graphene.

PACS: **73.22.-f,71.70.Ej,78.20.Ci**

The layered condensed-matter systems have become one the main-stream materials, as they possess the unusual lattice symmetries and the nano-scaled thickness. Such emergent 2D systems are very suitable in exploring the diverse physical, chemical, and material fundamental properties, especially for monoelemental graphene [1, 2], silicene [3, 4], germanene [5, 6], tinene [7], phosphorene [8, 9], antimonene [10, 11] and bismuthene [12, 13, 14, 15]. Recently, few-layer bismuthene could be directly obtained from the mechanical exfoliation, as used for graphene systems in 2004 [1]. Furthermore, they are successfully synthesized on the 3D $\text{Bi}_2\text{Te}_3(111)/\text{Bi}_2\text{Se}_3(111)/\text{Si}(111)$ substrates [14, 15, 16, 17]. The electronic and optical properties are easily tuned by the perpendicular electric field ($F_z\hat{z}$), owing to the highly buckled structure. This work is focused on absorption spectra of monolayer bismuthene in the absence and presence of F_z .

A rhombohedral bismuth is a well-known semimetal, being similar to the semi-metallic ABC-stacked graphite. However, the intrinsic inetrations are quite different from each other because of the significant spin-orbital coupling (SOC) in the former. When it becomes a 2D bismuthene [17, 18, 19, 20] or a 1D quantum wire [19, 21], the semi-metallic behavior is changed into the semiconducting property. There exist some theoretical and experimental studies on the geometric symmetries [17, 18, 19, 20], energy bands [18, 19, 20, 22], and transport properties [13]. The buckled structure is clearly identified by the measurements of scanning tunneling microscopy [16] and high-resolution electron diffraction[17, 22].

For monolayer bismuthene, the tight-binding model and the gradient approximation are, respectively, available in exploring the electronic and optical properties without/with $F_z\hat{z}$. Monolayer bismuthene consists of the buckled A and B sublattices with a separation of $l_z = 1.84 \text{ \AA}$, as shown in Fig. 1(a), in which the (x, y) -plane projections are the honeycomb

lattice with the primitive unit vectors \vec{a}_1 and \vec{a}_2 ($|\vec{a}_1| = 4.33 \text{ \AA}$). The buckling degree is characterized by the angle ($\theta = 126^\circ$) between the $Bi - Bi$ bond and z -axis (Fig. 1(b)). The low-lying Hamiltonian is built from the sp^3 bonding of the $6s$, $6p_x$, $6p_y$, and $6p_z$ orbitals in the presence of significant SOC:

$$H = \sum_{\langle i \rangle, o, s} E_o C_{ios}^+ C_{ios} + \sum_{\langle i, j \rangle, o, o', s} \gamma_{oo'}^{\vec{R}_{ij}} C_{ios}^+ C_{jo's} + \sum_{\langle \langle i, j \rangle \rangle, o, o', s} \gamma_{oo'}^{\vec{R}_{ij}} C_{ios}^+ C_{jo's}$$

$$+ \sum_{\langle i \rangle, p_\alpha, p_\beta, s, s'} \frac{\lambda_{soc}}{2} C_{ip_\alpha s}^+ C_{ip_\beta s'} (-i \epsilon_{\alpha\beta\gamma} \sigma_{ss'}^\gamma) + l_z \sum_{\langle i \rangle, o, s} F_z C_{ios}^+ C_{ios}, \quad (1)$$

which E_o of the $6s$ and $6p$ orbitals are, -9.643 eV and -0.263 eV , respectively [23]. The second term is the nearest-neighbor hopping integral $\gamma_{oo'}^{\vec{R}_{ij}}$, relying on the type of atomic orbitals, the vector between two atoms (\vec{R}_{ij}), and θ . The various interactions in the sp^3 bondings are $V_{pp\pi} = -0.679 \text{ eV}$, $V_{pp\sigma} = 2.271 \text{ eV}$, $V_{sp\sigma} = 1.3 \text{ eV}$, and $V_{ss\sigma} = -0.703 \text{ eV}$, as clearly indicated in Fig. 1(c). The next-nearest-neighbor hopping integrals in the third term, being independent of θ , cover $V_{pp\pi} = 0.004 \text{ eV}$, $V_{pp\sigma} = 0.303 \text{ eV}$, $V_{sp\sigma} = 0.065 \text{ eV}$, and $V_{ss\sigma} = -0.007 \text{ eV}$. The last term stands for the intra-atomic SOC, $V_{soc} = \lambda_{soc} \vec{L} \cdot \vec{s}$ ($\lambda_{soc} = 1.5 \text{ eV}$). α , β , and γ denote the x , y or z coordinates, and σ is the Pauli spin matrix. It could alter the spin configurations between the $6p_z$ and $(6p_x, 6p_y)$ orbitals & the $6p_x$ and $6p_y$ orbitals. The final term is the Coulomb potential energy due to an electric field F_z . When monolayer bismuthene exists in an electromagnetic wave, the occupied valence states are excited to the unoccupied conduction ones with the same wave vector. The electric dipole moment will induce the vertical optical excitations, in which the spectral intensity under the Fermi golden rule is characterized by

$$\begin{aligned}
A(\omega) \propto & \sum_{v,c,n,n'} \int_{1^{st}BZ} \frac{dk_x dk_y}{(2\pi)^2} \text{Im} \left[\frac{1}{E_{n'}^c(k_x, k_y) - E_n^v(k_x, k_y) - (\omega + i\gamma)} \right] \\
& \times \left| \langle \Psi_{n'}^c(k_x, k_y) | \frac{\vec{E} \cdot \vec{P}}{m_e} | \Psi_n^v(k_x, k_y) \rangle \right|^2,
\end{aligned} \tag{2}$$

where γ ($=10$ meV) is the broadening parameter due to various deexcitations and n represents the number of energy subbands, measured from the Fermi level. The electric polarization is in the \hat{x} -/ \hat{y} -direction. The absorption spectrum depends on the joint density of states (JDOS) between the valence and conduction states and the square of the velocity matrix element. The former is associated with energy dispersions or DOS while the latter is evaluated from the gradient approximation, being successfully utilized in graphene-related systems [24, 25, 26, 27].

Monolayer bismuthene possesses three low-lying energy bands (Fig. 2(a)), with two valence and one conduction bands centered about the Γ point. The first conduction band (c_1) has parabolic dispersions near the Fermi level along any directions, as observed in the second valence band (v_2). A sombrero-shaped energy dispersion, with the constant-energy loop, is revealed in the first valence band (v_1) with the local extremum deviating from Γ , so it could also be regarded as the 1D parabolic band. This is responsible for an indirect energy gap of $E_g^i = 0.295$ eV. The double spin degeneracy is clearly destroyed by an electric field under the z -plane mirror asymmetry. The spin-up- and spin-down-dominated energy bands are similar to each other, in which the extremal points are situated at/near the Γ point. With the increase of F_z , the conduction and valence bands approach to the Fermi level until the critical field strength of $F_{zc} = 0.82$ V/ \AA and then deviate from it. Energy gap diminishes to zero and opens again during the variation of F_z . Specifically, the linear Dirac-cone structures could be formed at F_{zc} , while the normal parabolic bands appear

beyond it.

DOS, as shown in Fig. 2(b), possess the special structures due to the van Hove singularities. The shoulder structures, the square-root asymmetric peaks, and the V-shaped form, respectively, arise from the local extremes, the constant-energy loops, and the linear Dirac cones in the energy-wave-vector space. The minimum/minima of the first conduction band exhibits an obvious step structure in the absence and presence of F_z . Apparently, its energy is very sensitive to the strength of F_z . It should be noticed that a step structure in the v_2 DOS becomes an asymmetric peak at sufficiently high field ($F_z \geq 0.4 \text{ V}/\text{\AA}$). However, one prominent peak of the v_1 DOS is changed into two peaks/the V-form/the step structures before/equal/beyond the critical field strength ($F_{zc} = 0.82 \text{ V}/\text{\AA}$), in which the higher-energy one is stronger compared with the lower-energy one. The predicted low-lying special structures in DOS could be directly verified by scanning tunneling microscopy [28, 29]. That will be directly reflected in optical absorption spectra. Monolayer bismuthene presents the unusual optical excitations (Fig. 3), being easily tuned by the external electric field in terms of the frequency, number, and intensity of special structures. There are prominent asymmetric peaks and shoulders arising from the JDOS. Without F_z , the threshold frequency is characterized by a strong asymmetric absorption peak (the red curve), so that the optical gap ($E_g^o = 0.35 \text{ eV}$) is different from the indirect band gap (0.295 eV). Specifically, it comes from constant-energy loop in the v_1 band and the corresponding c_1 conduction states with the same wave vectors. Moreover, an obvious shoulder appears at higher frequency of $\omega_s \sim 0.52 - 0.53 \text{ eV}$. The initial peak is split into two peaks with the lower intensities as F_z gradually grows (the blue, black, and black-squared blue curves), especially for the lowest threshold one. The splitting spectrum is accompanied with the decrease of optical

gap, in which the vanishing threshold frequency and the featureless spectrum could occur at the critical field. Beyond F_{zc} , the initial peak structures become a shoulder structure (the pink-triangled black curve). On the other hand, absorption frequency of shoulder structure might decline. This structure could be merged with the prominent peak and it would disappear near F_{zc} , or a shoulder structure is recovered beyond F_{zc} . The absence of absorption structure is revealed in the range of $0.6 \text{ V/}\text{\AA} \leq F_z \leq F_{zc}$.

The spectral intensity strongly depends on the strength of electric field, being very useful in fully understanding the absorption features and the comparison with the experimental measurements. The optical threshold frequency is determined by the lowest absorption boundary. E_g^o nonlinearly declines with the increase of F_z , becomes zero at F_{zc} , and then gradually increases in the further increment of F_z . Apparently, the second absorption structure split from the first one at $F_z = 0$ gradually approaches to the third one. Both of them are merged together at $F_z = 0.52 \text{ V/}\text{\AA}$, and the merged structure disappears at F_{zc} . Finally, a new absorption structure occurs at the higher frequency beyond F_{zc} . In short, monolayer bismuthene might possess three, two, one and zero absorption structures, and they are easily tuned by the electric field because of the significant buckled geometry.

The above-mentioned features of absorption spectra could be examined by various optical spectroscopies, such as the absorption, transmission, reflection, Raman scattering and Rayleigh scattering spectroscopies. They are successfully utilized to identify the low-frequency optical excitations in AB- and ABC-stacked trilayer graphenes [30, 31, 32]. For the former, the special shoulder structure at $\omega \sim 0.5 \text{ eV}$, which is induced by the band-edge state transitions from the parabolic valence band to the similar conduction band of another pair (not the same pair), is identified by the infrared reflection and absorp-

tion spectroscopies [24, 25, 26]. Recently, the similar optical measurements have verified the low-frequency optical properties, showing a clear evidence of two characteristic peaks associated with the surface-localized flat and sombrero-shaped energy bands [33]. The experimental examinations on the predicted low-frequency optical excitations will be very useful in exploring the effects due to the geometric symmetry, the intrinsic interactions, the spin-orbital coupling, and the external field. Monolayer bismuthene exhibits the unusual electronic and optical properties, being in sharp contrast to the linear Dirac-cone structure near the K/K' point without the featured absorption spectrum in monolayer graphene [34]. The low-lying c_1 , v_1 and v_2 bands are centered about/near the Γ point. The former two have an indirect gap of ~ 0.295 eV but an optical gap of ~ 0.35 eV. They show the threshold asymmetric peak and the higher-frequency shoulder, corresponding to $v_1 \rightarrow c_1$ and $v_2 \rightarrow c_1$ associated with the constant-energy loop and the parabolic extremum, respectively. The initial strong peak becomes two ones as F_z gradually increases. The step structure might be changed into the observable peak at sufficiently large F_z . The frequency, number, intensity, and form of optical spectra dramatically alter during the variation of F_z .

ACKNOWLEDGMENT

We thank Feng-Chuan Chuang for helpful discussions. This work is supported by the Ministry of Science and Technology of Taiwan, under grant Nos. MOST 105-2112-M-006-007-MY3, MOST-104-2112-M-110-002-MY3, and the support under NSYSU-NKMU Joint Research Project Nos. 105-P005 and 106-P005.

References

- [1] K. S. Novoselov, A. K. Geim, S. V. Morozov, D. Jiang, Y. Zhang, S. V. Dubonos, I. V. Grigorieva, and A. A. Firsov, *Science* **306**, 666 (2004).
- [2] K. S. Kim, Y. Zhao, H. Jang, S. Y. Lee, J. M. Kim, K. S. Kim, J. H. Ahn, P. Kim, J. Y. Choi, and B. H. Hong, *Nature* **457**, 706 (2009).
- [3] P. Vogt, P. D. Padova, C. Quaresima, J. Avila, E. Frantzeskakis, M. C. Asensio, A. Resta, B. Ealet, and G. L. Lay, *Phys. Rev. Lett.* **108**, 155501 (2012).
- [4] L. Tao, E. Cinquanta, D. Chiappe, C. Grazianetti, M. Fanciulli, M. Dubey, A. Molle, and D. Akinwande, *Nat. Nanotech.* **10**, 227 (2015).
- [5] L. Li, S. Z. Lu, J. Pan, Z. Qin, Y. Q. Wang, Y. Wang, G. Y. Cao, S. Du, and H. J. Gao, *Adv. Mater.* **26**, 4820 (2014).
- [6] M. Derivaz, D. Dentel, R. Stephan, M. C. Hanf, A. Mehdaoui, P. Sonnet, and C. Pirri, *Nano Lett.* **15**, 2510 (2015).
- [7] F. F. Zhu, W. J. Chen, Y. Xu, C. L. Gao, D. D. Guan, C. H. Liu, D. Qian, S. C. Zhang, and J. F. Jia, *Nat. Mater.* **14**, 1020 (2015).
- [8] L. Li, Y. Yu, G. J. Ye, Q. Ge, X. Ou, H. Wu, D. Feng, X. H. Chen, and Y. Zhang, *Nat. Nanotechnol.* **9**, 372 (2014).
- [9] P. Yasaeei, B. Kumar, T. Foroozan, C. Wang, M. Asadi, D. Tusche, J. E. Indacochea, R. F. Klie, and A. Salehi-Khojin, *Adv. Mater.* **27**, 1887 (2015).

[10] P. Ares, F. Aguilar-Galindo, D. Rodríguez-San-Miguel, D. A. Aldave, S. Díaz-Tendero, M. Alcamí, F. Martín, J. Gómez-Herrero, and F. Zamora, *Adv. Mater.* **28**, 6332 (2016).

[11] J. Ji, X. Song, J. Liu, Z. Yan, C. Huo, S. Zhang, M. Su, L. Liao, W. Wang, Z. Ni, Y. Hao, and H. Zeng, *Nat. Commun.* **7**, 13352 (2016).

[12] Z. F. Wang, M. Y. Yao, W. Ming, L. Miao, F. Zhu, C. Liu, C.L. Gao, D. Qian, J. F. Jia, and F. Liu, *Nat. Commun.* **4**, 1384 (2013).

[13] C. Sabater, D. Gosálbez-Martínez, J. Fernández-Rossier, J. G. Rodrigo, C. Untiedt, and J. J. Palacios, *Phys. Rev. Lett.* **110**, 176802 (2013).

[14] T. Hirahara, T. Nagao, I. Matsuda, G. Bihlmayer, E. V. Chulkov, Y. M. Koroteev, P. M. Echenique, M. Saito, and S. Hasegawa, *Phys. Rev. Lett.* **97**, 146803 (2006).

[15] T. Hirahara, T. Shirai, T. Hajiri, M. Matsunami, K. Tanaka, S. Kimura, S. Hasegawa, and K. Kobayashi, *Phys. Rev. Lett.* **115**, 106803 (2015).

[16] F. Yang, L. Miao, Z. F. Wang, M.-Y. Yao, F. Zhu, Y. R. Song, M.-X. Wang, J.-P. Xu, A. V. Fedorov, Z. Sun, G. B. Zhang, C. Liu, F. Liu, D. Qian, C. L. Gao, and J.-F. Jia, *Phys. Rev. Lett.* **109**, 016801 (2012).

[17] T. Hirahara, N. Fukui, T. Shirasawa, M. Yamada, M. Aitani, H. Miyazaki, M. Matsunami, S. Kimura, T. Takahashi, S. Hasegawa, and K. Kobayashi, *Phys. Rev. Lett.* **109**, 227401 (2012).

[18] Y. M. Koroteev, G. Bihlmayer, E. V. Chulkov, and S. Blugel, *Phys. Rev. B* **77**, 045428 (2008).

[19] J. Lee, W.-C. Tian, W.-L. Wang, and D.-X. Yao, *Sci. Rep.* **5**, 11512 (2015).

- [20] E. Akturk, O. Uzengi Akturk, and S. Ciraci, Phys. Rev. B **94**, 014115 (2016).
- [21] T. Hirahara, G. Bihlmayer, Y. Sakamoto, M. Yamada, H. Miyazaki, S. Kimura, S. Blugel, and S. Hasegawa, Phys. Rev. Lett. **107**, 166801 (2011).
- [22] N. Fukui, T. Hirahara, T. Shirasawa, T. Takahashi, K. Kobayashi, and S. Hasegawa, Phys. Rev. B **85**, 115426 (2012).
- [23] J. H. Xu, E. G. Wang, C. S. Ting, and W. P. Su, Phys. Rev. B **48**, 17271 (1993).
- [24] Z. Q. Li, E. A. Henriksen, Z. Jiang, Z. Hao, M. C. Martin, P. Kim, H. L. Stormer, and D. N. Basov, Nat. Phys., **4**, 532 (2008).
- [25] L. M. Zhang, Z. Q. Li, D. N. Basov, M. M. Fogler, Z. Hao, and M. C. Martin, Phys. Rev. B, **78**, 235408 (2008).
- [26] A. B. Kuzmenko, E. van Heumen, D. van der Marel, P. Lerch, P. Blake, K. S. Novoselov, and A. K. Geim, Phys. Rev. B **79**, 115441 (2009).
- [27] Y. H. Lai, J. H. Ho, C. P. Chang, and M. F. Lin, Phys. Rev. B **77**, 085426 (2008).
- [28] Y. Niimi, T. Matsui, H. Kambara, K. Tagami, M. Tsukada, and H. Fukuyama, Phys. Rev. B **73**, 085421 (2006).
- [29] J. A. Stroscio, R. M. Fccnstra, and A. P. Fein, Phys. Rev. Lett. **57**, 2579 (1986).
- [30] C. L. Lu, C. P. Ho, C. P. Chang, Y. C. Huang, R. B. Chen, and M. F. Lin, Phys. Rev. B **73**, 144427 (2006).
- [31] C. W. Chiu and R. B. Chen, Appl. Phys. Express, **9**, 065103 (2016).

[32] C. Y. Lin, J. Y. Wu, Y. J. Ou, Y. H. Chiu, and M. F. Lin, *Phys. Chem. Chem. Phys.* **17**, 26008 (2015).

[33] K. F. Mak, J. Shan, and T. F. Heinz, *Phys. Rev. Lett.* **104**, 176404 (2010).

[34] D. S. L. Abergel and V. I. Falko, *Phys. Rev. B* **75**, 155430 (2007).

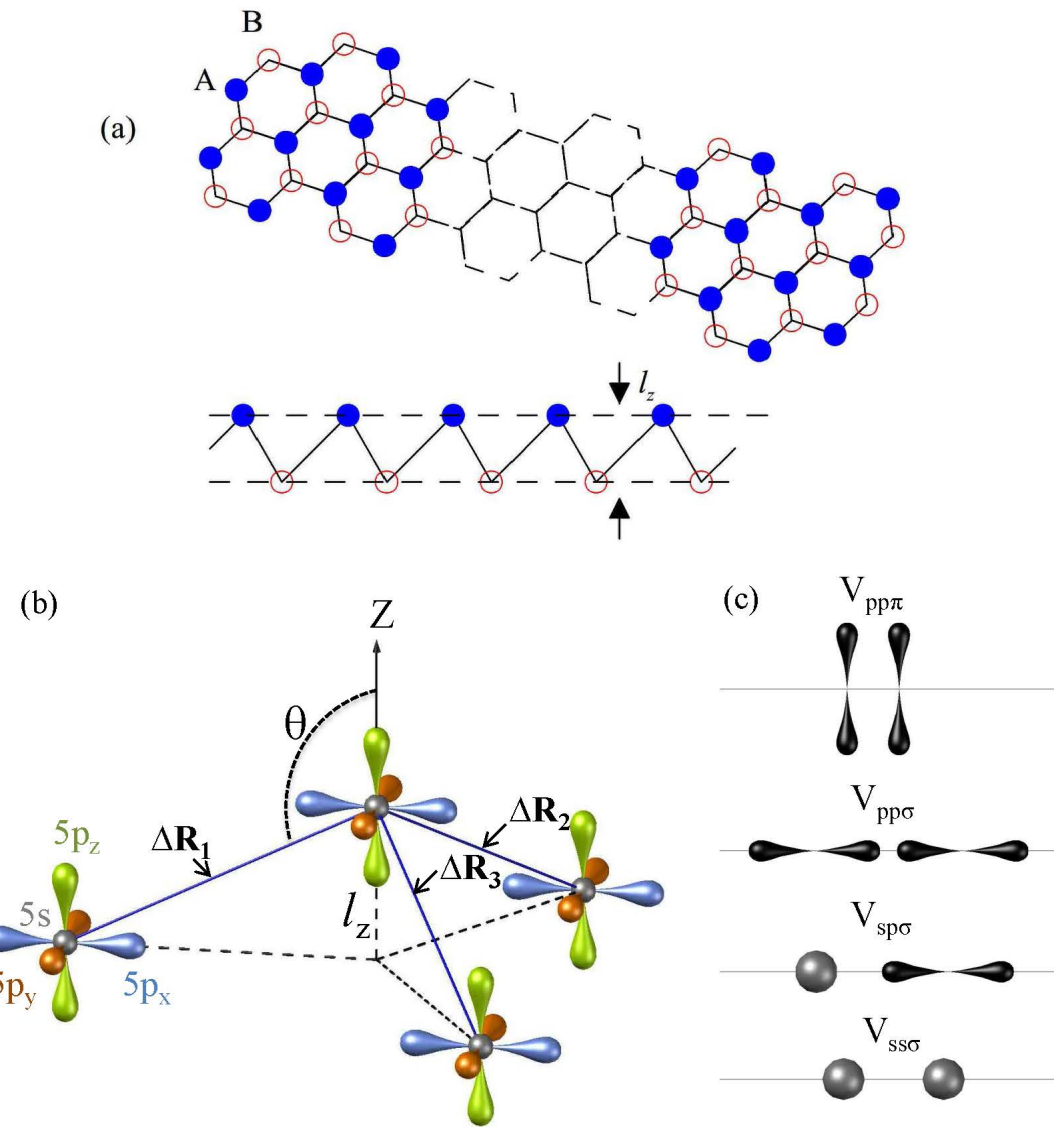


Figure 1: (a) the top and side views of monolayer bismuthene, (b) the sp^3 orbital hybridizations, and (c) the various π and σ bondings.

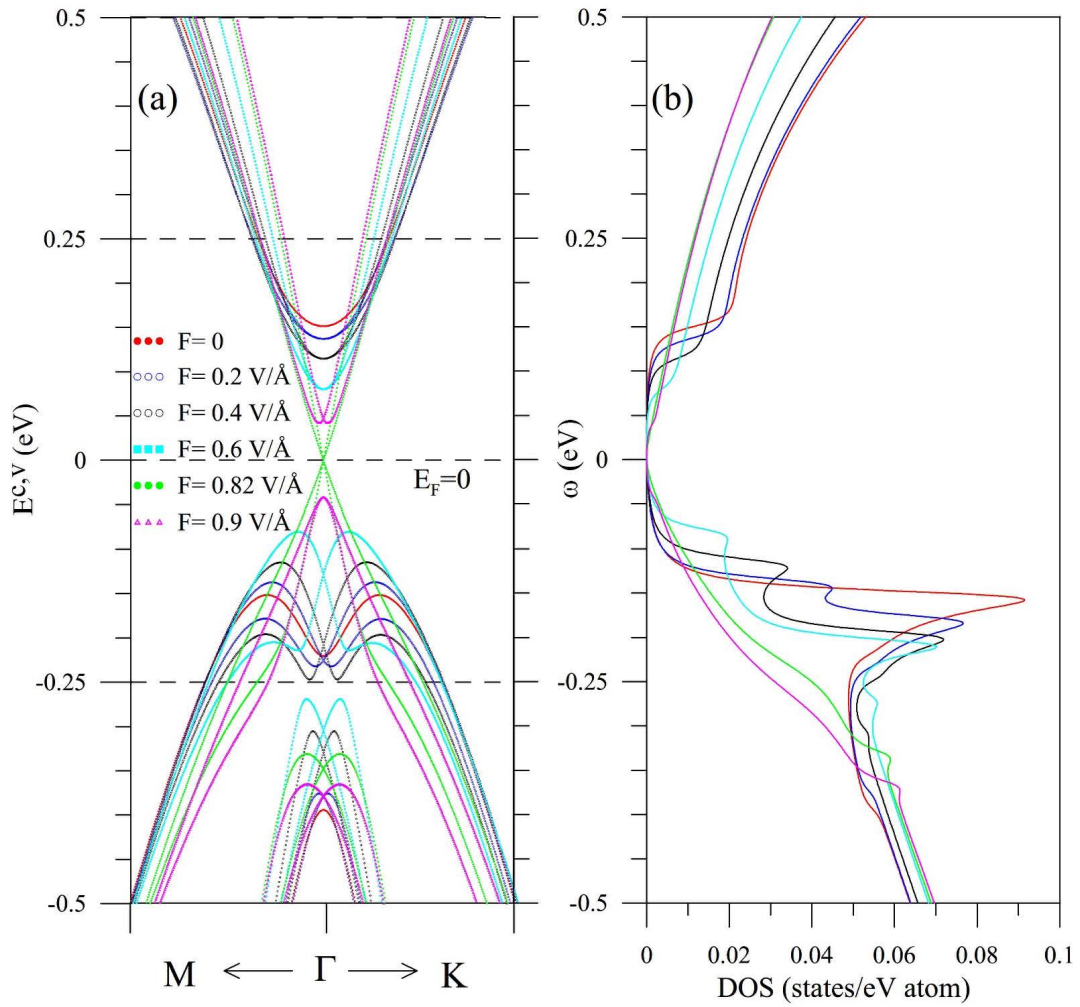


Figure 2: The low-lying (a) band structures and (b) densities of states of monolayer bismuthene at distinct electric fields.

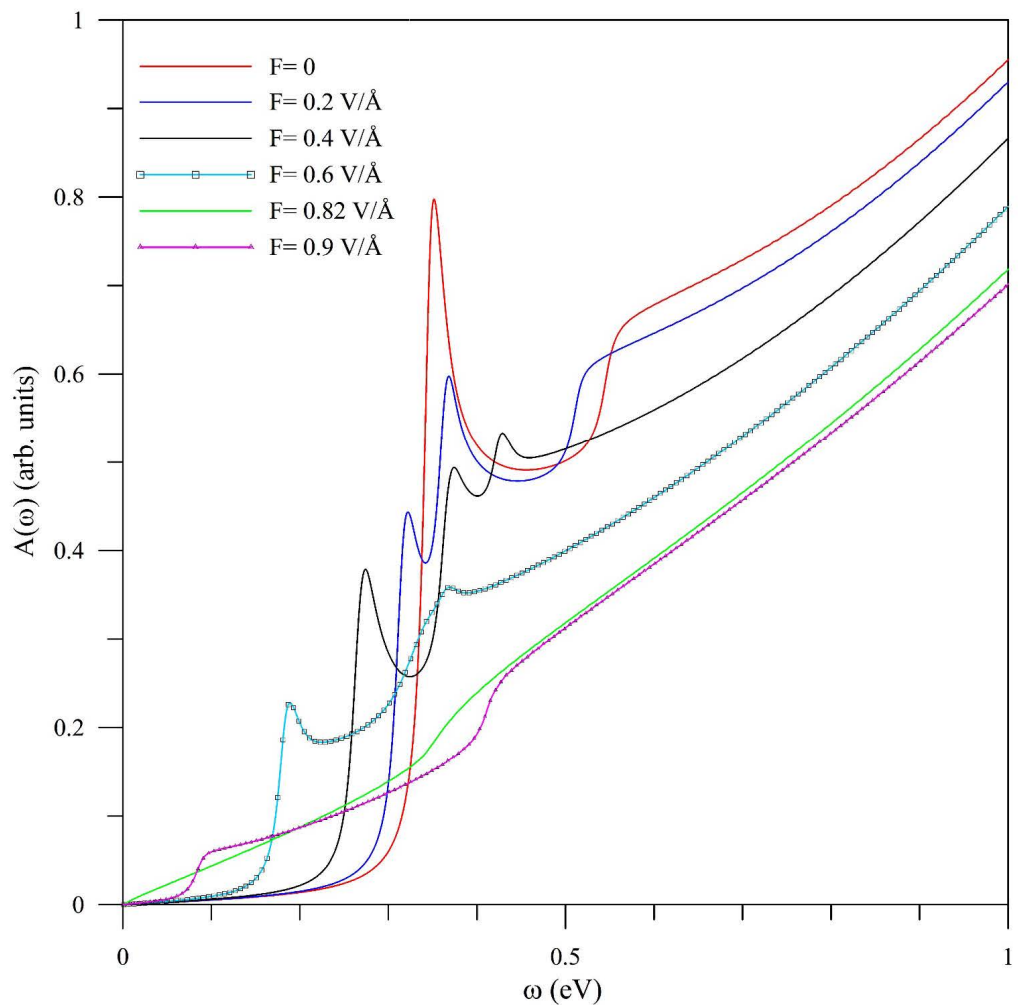


Figure 3: The optical absorption spectra of monolayer bismuthene under the various electric fields.

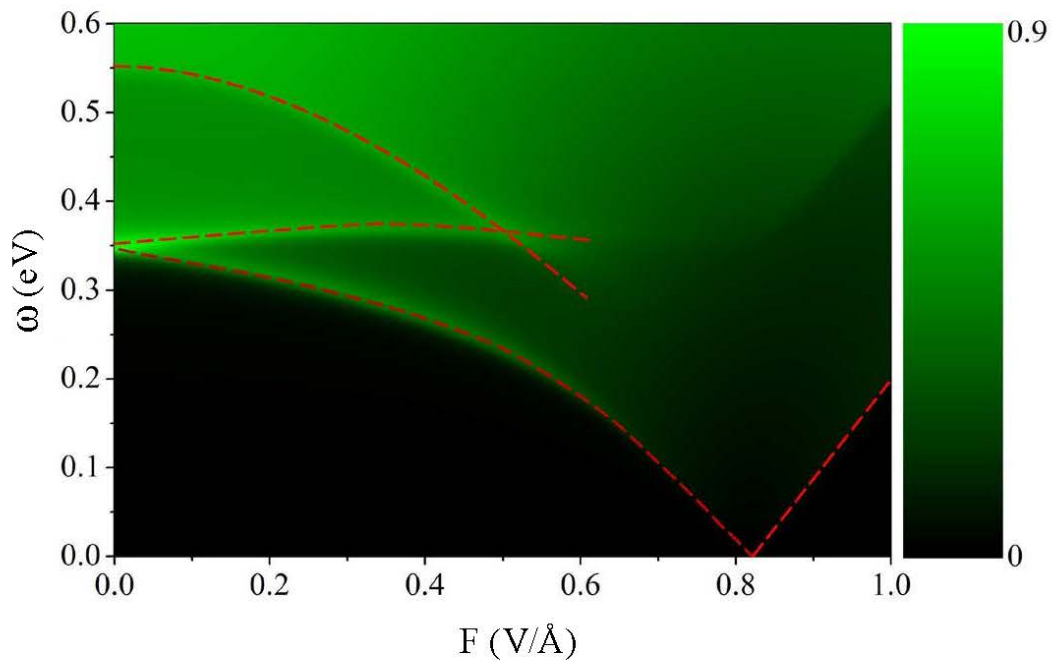


Figure 4: The electric-field-dependent spectral intensities, with the absorption structures indicated by the red dashed curves.